Aurivillius phases of $PbBi_4Ti_4O_{15}$ doped with Mn^{3+} synthesized by molten salt technique: Structure, dielectric, and magnetic properties

Zulhadjri [a,1], B. Prijamboedi [a], A.A. Nugroho [b], N. Mufti [c], A. Fajar [d], T.T.M. Palstra [e], Ismunandar [a,*]

[a] Inorganic and Physical Chemistry Group, Faculty of Mathematics and Natural Sciences, Institut Teknologi Bandung, Jl. Ganesha No. 10, Bandung, Indonesia
[b] Magnetic and Photonic Physics Research-Group, Faculty of Mathematics and Natural Sciences, Institut Teknologi Bandung, Jl. Ganesha No. 10, Bandung, Indonesia
[c] Physics Department, Universitas Negeri Malang, Jl. Surabaya 6, Malang 65145, Indonesia
[d] Centre for Technology of Nuclear Industry Materials – BATAN Puspiptek Serpong, Tangerang, Indonesia
[e] Solid State Materials Laboratory, Zernike Institute for Advanced Materials, Rijksuniversiteit Groningen, Nijenborgh 4, 9747AG Groningen, The Netherlands

ARTICLE INFO

ABSTRACT

Doping of manganese (Mn^{3+}/Mn^{4+}) into the Aurivillius phase $Pb_{1-x}Bi_{4+x}Ti_{4-x}Mn_xO_{15}$ was carried out using the molten salt technique for various Mn concentrations ($x=0$, 0.2, 0.4, 0.6, 0.8, and 1). Single phase samples could be obtained in the composition range with x up to 0.6 as confirmed by X-ray and neutron diffraction analysis. Dielectric measurements show a peak at 801, 803, 813 and 850 K for samples with $x=0$, 0.2, 0.4, and 0.6, respectively, related to the ferroelectric transition temperature (T_c). The main contribution of the in-plane polarization for $x \leq 0.2$ which was calculated from the atomic positions obtained by the structure analysis is the dipole moment in the $Ti(1)O_6$ layer; however, for $x \geq 0.4$ the polarization originates from the dipole moment in the $Ti(2)O_6$ layer. Mn doping in the $Pb_{1-x}Bi_{4+x}Ti_{4-x}Mn_xO_{15}$ does not show any long range magnetic ordering.

© 2011 Elsevier Inc. All rights reserved.

1. Introduction

The Aurivillius phases are a class of layered bismuth oxides, which can be described structurally as intergrowths of fluorite-like $[Bi_2O_2]^{2+}$ layers and n perovskite-type layers $[A_{n-1}B_nO_{3n+1}]^{2-}$ [1]. Generally, the A-site is occupied by mono-, di- or tri-valent cations that have dodecahedral coordination, whereas the B-site is occupied by a transition element with octahedral coordination, n is an integer representing the number of sheets of corner-sharing BO_6 octahedra forming the ABO_3-type perovskite blocks. Most of these phases have been known as ferroelectric materials with high Curie temperatures, T_c, such as $Bi_4Ti_3O_{12}$ (948 K), $PbBi_4Ti_4O_{15}$ (843 K), and $Pb_2Bi_4Ti_5O_{18}$ (583 K) [2,3]. The perovskite layer is considered to be responsible for the ferroelectricity due to the presence of d^0 transition cation such as Ti^{4+}. The introduction of magnetic transition metal cations (d^n) into the perovskite layers in the Aurivillius phases has received much interest since this may result in a material which has both dielectric and magnetic properties. Several Aurivillius phases containing both of d^0 and d^n cations, such as $Bi_5Ti_3FeO_{15}$ and $Bi_6Ti_3Fe_2O_{18}$ have been synthesized, studied and reported [4–6].

These Aurivillius compounds could be obtained in single phase; and were found to be ferroelectric with antiferromagnetic correlations. However, to obtain the Aurivillius with both ferroelectric and ferromagnetic ordering is still not managed. It was reported that the perovskite $BiMnO_3$ has a monoclinic ($C2$) structure with a Curie temperature for ferroelectricity at 470 K and ferromagnetism transition at 100 K [7]. Therefore, the introduction of Mn^{3+} into a perovskite block is expected to yield a material that has interesting properties, including combined ferroelectricity and ferromagnetism in a single phase.

Preparation of the Aurivillius phase with d^0 and d^n ions by conventional solid state reaction is very difficult [8]. The presence of different valency ions can lead to the formation of other phases. The conventional solid state reaction method also has other disadvantages such as a low homogeneity of the mixture of reactants and slow ionic diffusion. In addition, bismuth oxides are relatively volatile and the reactivity among Ti^{4+} or Nb^{5+} and Mn^{3+} in solids is different. These could lead to compositional changes or defects in the Bi_2O_2 layers. Synthesis of the perovskite $BiMnO_3$ is difficult because it has a highly distorted structure with a metastable phase. Therefore, high pressure is the only known method to prepare monoclinic $BiMnO_3$ [7]. Some Aurivillius phases containing both Ti^{4+} or Nb^{5+} and Mn^{3+} cations synthesized by solid-state reaction have been reported [9–13]. However, the presence of impurities in the samples was a common problem in all of these studies. There are also conflicting reports on the

---

* Corresponding author. Fax: +62 022 250 4154.
   E-mail address: ismu@chem.itb.ac.id (Ismunandar).
   [1] Permanent address: Chemistry Department, Faculty of Mathematics and Natural Sciences, Universitas Andalas, Kampus Limau Manis, Padang 25163, Indonesia.

Aurivillius phases prepared by conventional solid state reaction. For example, Yu et al. [9] reported that they successfully prepared $Bi_2Sr_2Nb_2MnO_{12-\delta}$, but McCabe and Greaves [10] cannot prepare this compound by the same method. Furthermore, Kumar et al. [11] and Suresh et al. [12] have reported the synthesis of $Bi_5Ti_3MnO_{15}$ and $Bi_6Ti_3Mn_2O_{18}$, respectively, by solid state reactions. However, the detailed structural properties of these compounds have not been reported. Information on the structure of these Aurivillius phases is very important in order to elucidate the nature of the ferroelectricity. The origin of the dipole moments that are responsible for ferroelectricty is also still unclear. Several authors have reported results of their studies in order to elucidate the origin of ferroelectricity in the Aurivillius phases from the crystal structure [14,15].

In recent years, unconventional methods, such as the molten salt flux technique, which provides high homogeneity in the mixture of the precursor, have been reported to be successful for synthesis of Aurivillius phases. Porob and Maggard [8] and Fuentes et al. [16] have applied this technique to produce magnetoelectric compounds of $Bi_5Ti_3FeO_{15}$ using Na_2SO_4/K_2SO_4 and NaCl/KCl as flux, respectively. The molten salt can act as a medium to facilitate the reactants to dissolve in order to get homogeneous mixing and high ionic mobility in the liquid phase [17]. It is assumed that the perovskite layer containing both Ti^{4+} and Mn^{3+} cations in the Aurivillius phases can be more easily prepared in a homogeneous mixture of a liquid phase.

Recently, we have reported the synthesis of the Aurivillius phases, $n=4$ containing magnetic and ferroelectric cations, $Pb_{1-x}Bi_{4+x}Ti_{4-x}Mn_xO_{15}$ with composition $0 \le x \le 1$ by the molten-salt method [18]. In this paper, we report the crystal structure of $Pb_{1-x}Bi_{4+x}Ti_{4-x}Mn_xO_{15}$ $(0 \le x \le 1)$ analyzed by X-ray and neutron powder diffraction, together with their dielectric and magnetic properties.

2. Experimental

Stoichiometric quantities of starting materials TiO_2, Mn_2O_3, Bi_2O_3, and PbO with high purity (Aldrich, $\ge 99.9\%$) were mixed in an agate mortar. The mixture of starting materials then was ground together with the mixture of Na_2SO_4/K_2SO_4 salts (1:1 molar ratio). The molar ratio of the oxide compounds to the salt mixture was 1:7, which means an excess in the salt mixture. The reactant mixtures were placed in an alumina crucible and heated to temperatures of 1023, 1123, and 1173 K for 15 h. Resulting products were washed several times using hot distilled water to remove the alkali salts and dried at 383 K for 24 h. Powder X-ray diffraction (XRD) data were collected on a Bruker D8 diffractometer using monochromatised CuKα radiation from $2\theta=10°$ to $100°$ with a step-size of $0.02°$ and a counting time of 7 s per step. Powder neutron diffraction (PND) data were collected on the Fine Resolution Powder Diffractometer (DN3) [19] at The Neutron Spectrometry Division of Center for Technology of Nuclear Industry Material-BATAN, Serpong, Indonesia. The wavelength of incident neutron beam was 1.8195 Å. The diffraction data were collected over the range of $2\theta=2.5–162.5°$ with a step size of $0.05°$. The Rietveld refinement of the neutron data was performed using the RIETICA program [20].

For the dielectric constant measurements, the powders were pressed into pellets with 10 mm in diameter and a thickness of about 1 mm. These pellets were sintered at 1073 K for 12 h in air for densification. We used electrodes from silver paste painted on both sides of the pellet and the painted pellet was heated at 473 K for 2 h. The dielectric properties of the samples were measured by using an LCR meter (Agilent 4980A) with drive voltage of 1 V in the temperature range of 300–873 K at different frequencies from 80 Hz to 2 MHz. The magnetization was measured using a SQUID magnetometer MPMS of Quantum Design in the temperature range from 2 to 300 K in a magnetic field of 1 T.

3. Results and discussion

The X-ray diffraction (XRD) data of $Pb_{1-x}Bi_{4+x}Ti_{4-x}Mn_xO_{15}$ powders with $x=0$, 0.2, 0.4, 0.6, 0.8 and 1 are shown in Fig. 1. In general, these patterns match with the XRD pattern of the Aurivillius phase with $n=4$ as reported in other papers [5,21,22] with an orthorhombic structure and space group $A2_1am$. Doping of Mn may cause local distortions that cannot be easily incorporated into the space group. However, it was not possible to get realistic refinement results using lower symmetry model. Powder samples with composition of $x=0$, 0.2, 0.4, and 0.6 formed single-phase Aurivillius compound, while the samples with $x=0.8$ and 1 showed additional phases. The additional phases were identified as $Bi_4Ti_3O_{12}$ [23] and $Bi_2Mn_4O_{10}$ [24]. Among the XRD patterns of the samples showed a single phase ($x=0$, 0.2, 0.4, and 0.6), the pattern for $x=0.2$ exhibits a strong preferred orientation in the $(0\ 0\ l)$ direction. The XRD patterns in Fig. 1 gave initial information that the maximum amount of Mn that can be doped into the Aurivillius phases $PbBi_4Ti_4O_{15}$ to form a single phase using the molten salt technique is around $x=0.6$.

In order to study the structure in detail, powder neutron diffraction (PND) data were obtained for the samples with $x=0.2$, 0.4, and 0.6, which are single phase, at room temperature. The Rietveld refinements for PND data were carried out initially with space group $A2_1am$ using the $PbBi_4Ti_4O_{15}$ structure as reported by Kennedy et al. [22] as a starting model. Refinements were carried out with a preferred orientation parameter along $[0\ 0\ l]$. The R-factor values and the refinement results are given in Table 1, while the fits are given in Fig. 2 for $x=0.2$, 0.4, and 0.6.

The lattice parameters and the volume of unit cells of single phase $Pb_{1-x}Bi_{4+x}Ti_{4-x}Mn_xO_{15}$ from the neutron diffraction measurement ($x=0$, 0.2, 0.4, and 0.6) are shown in Fig. 3. The data for $x=0$ were taken from Kennedy et al. [22] and we also use the data for further analysis. The lattice constants a and b are relatively the same for $x=0$, 0.2, and 0.6 and slightly lower for $x=0.4$; the lattice constant c decreases with increasing x. The volume of unit cell decreases up to $x=0.6$. This indicates that the limit of Mn concentration that can be introduced to form single phase of Aurivillius is up to $x=0.6$. These results agree well with the XRD results described above. As expected, the unit cell volume decreases as the Mn-concentration increases since the cationic radius of Bi^{3+} (1.17 Å) [25] is smaller than Pb^{2+} (1.29 Å) while the ionic radii of Ti^{4+} (0.605 Å) is nearly the same as Mn^{3+} (0.645 Å). It was found that replacing completely Ti^{4+} by Mn^{3+} is difficult, since they have
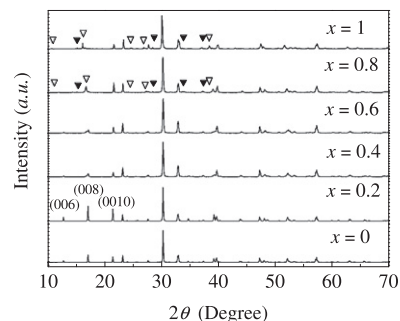

Fig. 1. Powder X-ray diffraction pattern of $Pb_{1-x}Bi_{4+x}Ti_{4-x}Mn_xO_{15}$ synthesized by the molten salt method: $\triangledown=Bi_4Ti_3O_{12}$ and $\blacktriangledown=Bi_2Mn_4O_{10}$. The sample with $x=0.2$ shows higher peaks for the $hkl=(0\ 0\ 6)$, $(0\ 0\ 8)$, and $(0\ 0\ 10)$ compared with other compounds that form single phase Aurivillius compounds ($x=0$, 0.4, and 0.6).

Table 1
Unit cell parameters of $Pb_{1-x}Bi_{4+x}Ti_{4-x}Mn_xO_{15}$ ($x=0.2$, 0.4, and 0.6) refined from neutron diffraction using the space group $A2_1am$.

Cell parameter	Sample $Pb_{1-x}Bi_{4+x}Ti_{4-x}Mn_xO_{15}$		
	$x=0.2$	$x=0.4$	$x=0.6$
a (Å)	5.4509(4)	5.4420(4)	5.4442(4)
b (Å)	5.4304(3)	5.4258(4)	5.4285(4)
c (Å)	41.340(2)	41.185(3)	41.109(3)
V (Å^3)	1223.7(1)	1216.1(2)	1214.9(2)
$b-a$ (Å)	−0.0205	−0.0162	−0.0157
c/a	7.584	7.568	7.551
Z	4	4	4
R_p (%)	11.40	10.91	11.29
R_{wp} (%)	14.95	13.98	14.87
χ^2	1.30	1.77	3.22
R_{Brag}	4.81	4.74	6.46
R_{exp}	13.11	10.51	8.28
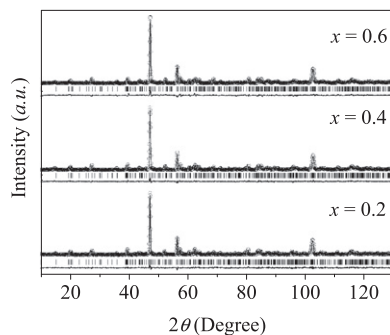
Fig. 2. Rietveld refinement of PND of $Pb_{1-x}Bi_{4+x}Ti_{4-x}Mn_xO_{15}$ with $x=0.2$, 0.4, and 0.6. Observed PND intensity (circle), calculated data (solid line), and the difference patterns, $y_{obs}-y_{cal}$ (solid line on the bottom curve). The tick marks represent the positions of allowed Bragg reflections in the space group $A2_1am$.
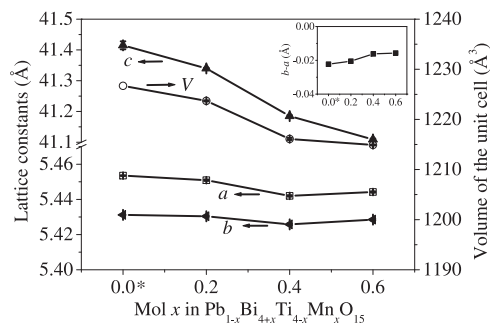

Fig. 3. Lattice constants and volume of the unit cell as a function of Mn content for $Pb_{1-x}Bi_{4+x}Ti_{4-x}Mn_xO_{15}$ with $0 \le x \le 0.6$. The inset shows the difference between the lattice parameters ($b-a$). $^*x=0$ data were from Kennedy et al. [22].

a different valency. The samples containing high Mn-concentration ($x=0.8$ and 1) tend to form the three-layered Aurivillius phase ($Bi_4Ti_3O_{12}$) and the $Bi_2Mn_4O_{10}$ phase. The inset of Fig. 3 shows the difference between the lattice parameters ($b-a$). The value of $b-a$ is constant for $x=0$ and 0.2 and slightly higher for $x=0.4$ and 0.6 (that are the same). Decreasing $|b-a|$ indicates a decreasing of the orthorombicity of these samples.

The atomic positions for the samples with $x=0.2$, 0.4, and 0.6 obtained from the final refinements are given in supplementary data. All atoms occupy the $8b$ site, except for Bi(1) and O(1) that occupy the $4a$ site. In these refinements, the Pb atoms are randomly distributed over the Bi(2) and Bi(3) sites; however, it was not possible to refine their occupancies. Also, it was not

possible to model any ordering between the Ti and Mn atoms. The B_{iso} values of Ti/Mn and some O atoms were fixed at reasonable values of 0.6, since it has not been possible to get a meaningful B_{iso} if they were refined. The atomic position, x for Bi(1) for all samples was fixed to define an origin of the polar axis.

The structure of $Pb_{1-x}Bi_{4+x}Ti_{4-x}Mn_xO_{15}$ ($x=0$, 0.2, 0.4, and 0.6) is shown in Fig. 4a. This figure also shows the position of the atoms forming octahedra in the perovskite layer (Fig. 4b). The center of the (MO_6) octahedra in the perovskite blocks is occupied by Ti or Mn. These octahedra form chains of O–(Ti)–O along the c-axis separated by $(Bi_2O_2)^{2+}$ layers. There are two types of octahedra, i.e. Ti(1)O_6 and Ti(2)O_6 and both exhibit significant distortion (tilting). The octahedral tilting in perovskites has been described by Glazer [26] and others [21,22,27]. The tilting of MO_6 octahedra has two possibilities, i.e. adjacent octahedra rotate all in the same sense (*in-phase*) or in the opposite sense (*out-of-phase*). As shown in Fig. 5, there are two types of TiO$_6$ octahedra in PbBi$_4$Ti$_4$O$_{15}$, i.e. inner Ti(1)O_6 and outer Ti(2)O_6 octahedra. The rotation of the adjacent octahedra Ti(1)O_6/Ti(1)O_6 and Ti(2)O_6/Ti(2)O_6 is *in-phase*, while the rotation of the Ti(1)O_6 and Ti(2)O_6 octahedra are *out-of-phase*.

We first focus on the atomic displacements in the perovskite block since it is believed to be responsible for ferroelectricity. The selected bond lengths between cation and anion for the samples with $x=0.2$, 0.4, and 0.6 are given in Fig. 5. In the Ti(1)O_6 octahedra, we observe that by introducing Mn into these octahedral, the bond lengths of Ti(1)–O(1) and Ti(1)–O(3), both along c-axis, are almost equal. Meanwhile in the ab plane, we observe that there are noticeable different bond lengths of Ti–O especially for $x<0.4$ and those Ti–O bond lengths tend to be equal at higher Mn concentration. For the Ti(2)O_6 octahedra, we found that the difference between the bond lengths of Ti(2)–O(3) and Ti(2)–O(5) are relatively constant as the Mn concentration increases. The bond length of Ti(2)–O(3) is longer than the bond length of Ti(2)–O(5) for all of x. Thus, the outer octahedra [Ti(2)O_6] have a structural distortion mainly along the c-axis, evidenced by the large difference in bond length of Ti(2)–O(3) and Ti(2)–O(5). The introduction of Mn into the Aurivillius phase
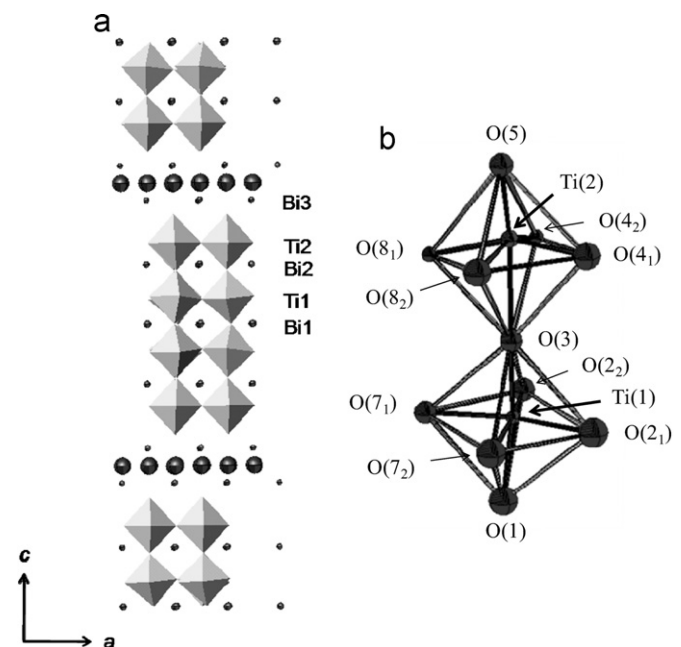

Fig. 4. (a) Representation of the structure of the $n=4$ Aurivillius oxide $Pb_{1-x}Bi_{4+x}Ti_{4-x}Mn_xO_{15}$ with $A2_1am$ space group, (b) the position of the atoms forming octahedra in the perovskite layer.
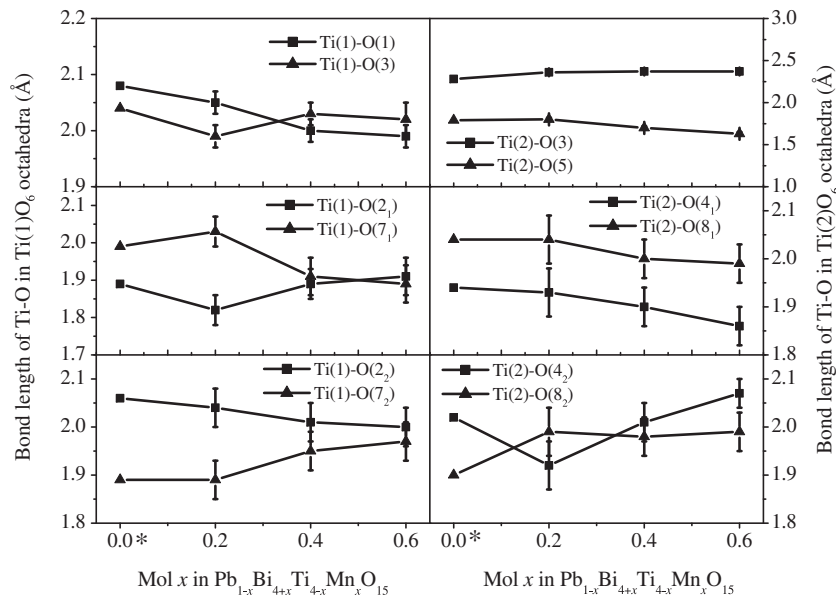
Fig. 5. Bond lengths of Ti–O in TiO$_6$ octahedra for Pb$_{1-x}$Bi$_{4+x}$Ti$_{4-x}$Mn$_x$O$_{15}$ with $x=0$, 0.2, 0.4, and 0.6. *$x=0$ data were from Kennedy et al. [22].

strongly indicate that Mn tends to retain the distortion of Ti(2)O$_6$. The outer Ti(2)O$_6$ octahedra are more distorted than the inner Ti(1)O$_6$. The same features, i.e. outer octahedral are more distorted than the inner ones, have been observed in other $n \geq 2$ Aurivillius phase [5,13,22]. The higher symmetric condition in Ti(1)O$_6$ give an indication that the Mn ions could mainly distributed at this site. We could explain as follows: the filled or partially filled d-orbitals of transition metal ions could easily hybridize with the O $2p$ orbitals [28] and this hybridization could lead to high symmetrical octahedra or similar bond length between Mn ion with oxygen ions at the opposite direction. The high symmetrical of Mn octahedra then would favor in residing in the inner TiO$_6$ octahedra since it has lowest distortion compared to the outer octahedra.

The temperature dependence of the dielectric constant for the Pb$_{1-x}$Bi$_{4+x}$Ti$_{4-x}$Mn$_x$O$_{15}$ ($x=0$, 0.2, 0.4, and 0.6) at various frequencies is depicted in Fig. 6. Here, we show the dielectric constant data measured at 600 kHz, 1, and 2 MHz. The samples with composition $x=0$, 0.2, and 0.4 exhibit peaks around 801, 803, and 813 K, respectively. The peak for $x=0$ is broad and is similar to the peak reported for the single crystal of PbBi$_4$Ti$_4$O$_{15}$ [29]. The broad peak, the ferroelectric ordering temperature (T_c), is attributed to the disorder of Pb and Bi atoms in the Bi$_2$O$_2$ layers and in the perovskite layers as described for PbBi$_2$Nb$_2$O$_9$ [30]. The (T_c) peaks of Pb$_{1-x}$Bi$_{4+x}$Ti$_{4-x}$Mn$_x$O$_{15}$ resemble the observations by Fernandez et al. [3] (808 K) and are slightly lower than the value reported by Subbarao [2] (843 K) and Ikezaki et al. [29] (823 K) both for composition of PbBi$_4$Ti$_4$O$_{15}$. However, the sample $x=0.6$ exhibits a peak at higher temperature (850 K). We can clearly observe that the transition for $x=0.2$ is sharper than for the other samples. This can be attributed to the smaller disorder of Pb and Bi atoms. Although, the occupancies of Pb and Bi atoms could not be refined, an indication of the disorder was observed in the peak widths. The FWHM calculated from the XRD data for the (0 0 6), (0 0 8), and (0 0 10) reflections for $x=0.2$ are around $\sim 0.082°$ and these are smaller than the FWHM for $x=0$, 0.4, and 0.6 with $\sim 0.083°$, $\sim 0.16°$, and $\sim 0.14°$, respectively. A smaller FWHM could indicate that the sample with $x=0.2$ has larger crystallite size compared than others; however, the scanning electron microscope images revealed that all samples have similar grain size. Therefore, we could expect that better crystallinity or
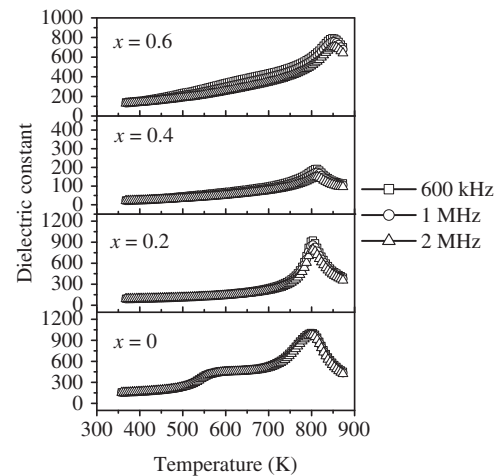

Fig. 6. Temperature dependence of dielectric constant of Aurivillius phases Pb$_{1-x}$Bi$_{4+x}$Ti$_{4-x}$Mn$_x$O$_{15}$ ($x=0$, 0.2, 0.4, and 0.6) for different frequencies.

ordering in the sample with $x=0.2$ and this would be responsible for sharp transition peak.

The dielectric constants of the Pb$_{1-x}$Bi$_{4+x}$Ti$_{4-x}$Mn$_x$O$_{15}$ shown in Fig. 6 are measured at high frequencies (≥ 600 kHz). At low frequencies (< 600 kHz), their dielectric constants have a high value and increase with increasing temperature, as shown in Fig. 7. From this figure, it can also be observed that the dielectric constant for all samples decreases with increasing frequency and become constant for frequency above 10 kHz. The increase of dielectric constant with decreasing frequency (≤ 10 kHz) can be caused by the interface of two electrically different regions of space charge (interfacial) polarization. The charge carriers accumulated on the interfaces between grains and at grain boundaries can lead to an increasing dielectric constant, known as Maxwell–Wagner effect [31]. Extrinsic factors, such as the formation of a thin layer between the contacts (electrodes) and the bulk (surface samples) are also another possible factors resulted in a high dielectric constant at low frequency. Therefore, we only use the data measured at high frequencies, since they can be related to the intrinsic polarizability of materials.
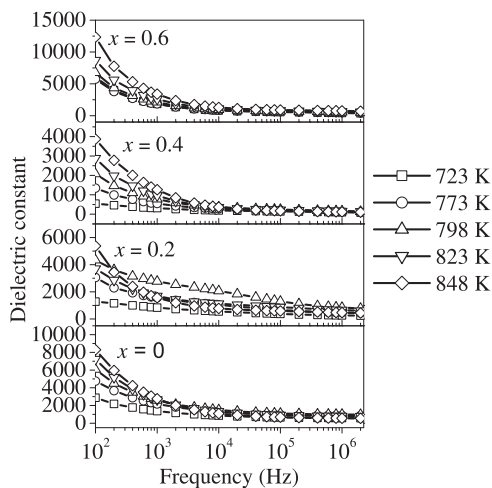
Fig. 7. Frequency dependence of the dielectric constant of Aurivillius phases $Pb_{1-x}Bi_{4+x}Ti_{4-x}Mn_xO_{15}$ ($x=0$, 0.2, 0.4, and 0.6) for different temperatures.
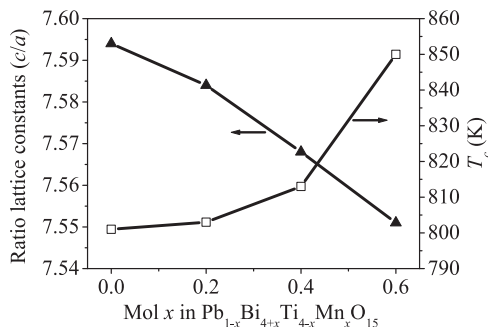

Fig. 8. Transition temperature (T_c) and c/a ratio as a function of x in $Pb_{1-x}Bi_{4+x}$-$Ti_{4-x}Mn_xO_{15}$ ($0 \leq x \leq 0.6$).

Fig. 9. The dipole moment of TiO_6 dependence of x in $Pb_{1-x}Bi_{4+x}Ti_{4-x}Mn_xO_{15}$ ($0 \leq x \leq 0.6$);); (a) along a-axis and (b) on the ab plane. *$x=0$ data were from Kennedy et al. [22].

Fig. 10. Temperature dependence of the magnetic susceptibility of the Aurivillius phases $Pb_{1-x}Bi_{4+x}Ti_{4-x}Mn_xO_{15}$ ($x=0$, 0.2, 0.4, and 0.6) as a function of temperature.

The transition temperature (T_c), determined from the dielectric constant measurements at high frequencies, are plotted versus Mn concentration in Fig. 8. In this figure, we observe that T_c increases slowly for $x \leq 0.2$ and then it increases sharply for $x \geq 0.4$. In the perovskite structures like $BaTiO_3$, the tetragonality or c/a ratio is related with the ferroelectric transition temperature. Larger c/a values yield ferroelectric distortions or polarizations. However, we observe that an increase of T_c is related with a decrease of the c/a ratio. This means that the ferroelectric distortion in this Aurivillius phase is different from that observed in the simple perovskite structure. In $A2_1am$ space group, the polarization in the c-axis could be ignored and a-axis direction plays an important role. Meanwhile, the existence of mirror and mirror glide planes perpendicular to the b-axis in $A2_1am$, prohibit the contribution of polarization in the b and c direction.

We now calculate the dipole moments of the TiO_6 octahedra in the samples in order to gain insight in the ferroelectricity of these compounds. The calculation is focused on the a-axis and the ab plane since as discussed above, the differences in bond lengths mainly occurred here and also considering the space group adopted by this system. Fig. 9 shows the calculated dipole moments total of TiO_6 octahedra from the structural data of $Pb_{1-x}Bi_{4+x}Ti_{4-x}Mn_xO_{15}$ with $x=0$, 0.2, 0.4, and 0.6 along the a-axis as well as the total dipole moment in the ab plane. The dipole moment along a-axis (Fig. 9a) and the ab plane (Fig. 9b) show an interesting feature. It is observed that the dipole moment of the $Ti(1)O_6$ octahedra in both are larger than the dipole moment of $Ti(2)O_6$ octahedra for $x \leq 0.2$ and the opposite situation was observed for samples with $x > 0.2$. It can be noted that the dipole moment from $Ti(1)O_6$ displacements is close to zero for

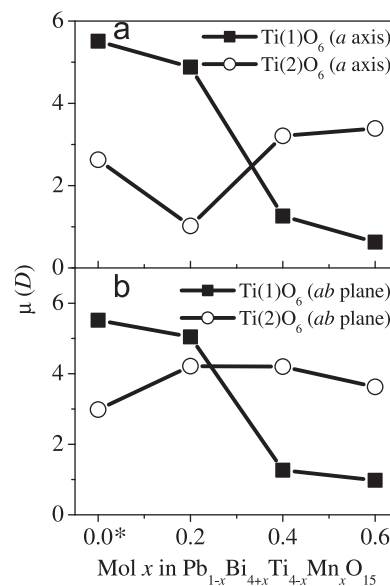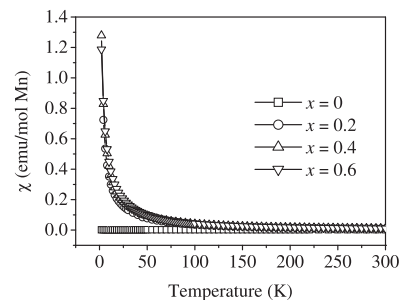$x \geq 0.4$, indicating a small contribution from this layer. In the Aurivillius phases with $Pb_xBi_4Ti_{3+x}O_{12+3x}$ series, the T_c is found to increase as the number of perovskite layer decreases [2,3]. Presumably increasing T_c in $Pb_{1-x}Bi_{4+x}Ti_{4-x}Mn_xO_{15}$ can be caused by a decrease of the contribution of the inner $Ti(1)O_6$ octahedra and a larger contribution of more distorted outer $Ti(2)O_6$ octahedra. Since we observed the behavior of dipole moments on the ab plane is similar to the a-axis, we could not ignore the contribution of dipole moments on the ab plane. As we mentioned before that the space group $A2_1am$, prohibit the contribution of polarization in b direction. The space group captures the global symmetry of the structure, but the Mn doping may lead to local displacements that violate this global symmetry. Thus it may possible that these could partially release the prohibition, and polarization in the ab-plane could contribute to the total polarization.

The magnetic susceptibility (χ) data versus temperature (T) for $Pb_{1-x}Bi_{4+x}Ti_{4-x}Mn_xO_{15}$ with $x=0$, 0.2, 0.4, and 0.6 are plotted in Fig. 10. All samples containing manganese ions exhibited paramagnetic behavior. The magnetic susceptibility of the samples increases with the concentration of Mn^{3+}. The susceptibility data were fitted by the Curie–Weiss equation; $\chi = \chi_0 + (C/(T-\theta))_{CW}$, where χ_0 is diamagnetic susceptibilityy, θ_{CW} is the Curie–Weiss temperature and C is the Curie constant. The fitting was performed in the temperature range above 175 K. The value of the Curie–Weiss temperature (θ_{CW}) is 1.51, 15.81, and 21.49 K and

Curie constant (C) is 3.72, 3.65, and 3.59 for $x=0.2$, 0.4, and 0.6, respectively. The Curie–Weiss temperature (θ) is positive for all samples indicating the presence of ferromagnetic interactions. Mn effective moments were derived from the Curie constant and calculated from; $\mu_{eff}=(8C)^{1/2}$. The result of Mn effective moment calculated from these sample is 5.46, 5.40, and 5.36 μ_B with $x=0.2$, 0.4, and 0.6, respectively. The Mn effective moment of $x=0.2$ is close to the free ion effective moment of Mn^{3+} (4.9 μ_B) while increasing Mn concentration give decreasing Mn effective moment indicating present of Mn^{4+} ($\mu_{eff}=3.87$ μ_B) besides Mn^{3+}. The interactions between Mn^{3+} and Mn^{4+} can prohibit polarization and render the sample more conducting.

4. Conclusion

The Aurivillius compounds of $Pb_{1-x}Bi_{4+x}Ti_{4-x}Mn_xO_{15}$ ($0 \leq x \leq 1$) have been prepared by the molten-salt technique. Single phase Aurivillius compounds with space group $A2_1am$ were found for the samples up to $x=0.6$. Meanwhile, the samples with $x \geq 0.8$ contained impurities identified as $Bi_4Ti_3O_{12}$ and $Bi_2Mn_4O_{10}$ phases. The result of neutron diffraction analysis revealed that the bond length of Ti–O in the perovskite layers becomes different with the introduction of Mn. A large change in bond length of Ti–O was observed for the inner $Ti(1)O_6$ which is found to be almost equal with increasing Mn concentration. The ferroelectric transition (T_c) was observed at the temperature 801, 803, 813 and 850 K for $x=0$, 0.2, 0.4, and 0.6, respectively. The T_c increases slowly for low x and more pronounced for $x > 0.2$. The increase of T_c can be related with reduced polarization of the inner $Ti(1)O_6$. The polarization that is predominantly responsible is given by the dipole moments of the inner $Ti(1)O_6$ octahedra for $x \leq 0.2$ and the dipole moment of the outer $Ti(2)O_6$ octahedra for $x > 0.2$. The ferromagnetic interactions in the paramagnetic show the contribution of mixed valence of Mn^{3+}/Mn^{4+}.

Acknowledgments

Appendix A. Supporting information

Supplementary data associated with this article can be found in the online version at doi:10.1016/j.jssc.2011.03.044.

References

[1] B. Aurivillius, Mixed bismuth oxides with layer lattices I, Ark. Kemi. 1 (54) (1949) 463–480.
[2] E.C. Subbarao, A family of ferroelectric bismuth compounds, J. Phys. Chem. Solids 23 (1962) 665–676.
[3] J.F. Fernandez, A.C. Caballero, M. Villegas, Relaxor behavior of $Pb_xBi_4Ti_{3+x}O_{12+3x}$ ($x=2$, 3) Aurivillius ceramics, Appl. Phys. Lett. 81 (25) (2002) 4811–4813.
[4] A. Srinivas, S.V. Suryanarayana, G.S. Kumar, M.H. Kumar, Magnetoelectric measurements on $Bi_5FeTi_3O_{15}$ and $Bi_6Fe_2Ti_3O_{18}$, J. Phys.: Condens. Matter 11 (1999) 3335–3340.
[5] C.H. Hervoches, A. Snedden, R. Riggs, S.H. Kicoyne, P. Manuel, P. Lightfoot, Structural behavior of the four-layer Aurivillius-phase ferroelectrics $SrBi_4Ti_4O_{15}$ and $Bi_5Ti_3FeO_{15}$, J. Solid State Chem. 164 (2002) 280–291.
[6] M. Garcia-Guaderrama, L.F. Montero, A. Rodriguez, L. Fuentes, Structural characterization of $Bi_6Ti_3Fe_2O_{18}$ obtained by molten salt synthesis, Integr. Ferroelectr. 83 (2006) 41–47.
[7] Z.H. Chi, C.J. Xiao, S.M. Feng, F.Y. Li, C.Q. Jin, Manifestation of ferroelectromagnetism in multiferroic $BiMnO_3$, J. Appl. Phys. 98 (2005) 103519-1–103519-5.
[8] D.G. Porob, P.A. Maggard, Synthesis of textures $Bi_5Ti_3FeO_{15}$ and $LaBi_4Ti_3FeO_{15}$ ferroelectric layered Aurivillius phases by molten-salt flux methods, Mater. Res. Bull. 41 (2006) 1513–1519.
[9] W.J. Yu, Y.I. Kim, D.H. Ha, J.H. Lee, Y.K. Park, S. Seong, N.H. Hur, A new manganese oxide with the Aurivillius structure: $Bi_2Sr_2Nb_2MnO_{12-\delta}$, Solid State Commun. 111 (1999) 707–709.
[10] E.E. McCabe, C. Greaves, Structural and magnetic characterisation of $Bi_2Sr_{1.4}La_{0.6}Nb_2MnO_{12}$ and its relationship to "$Bi_2Sr_2Nb_2MnO_{12}$", J. Mater. Chem. 15 (2005) 177–182.
[11] M.M. Kumar, A. Srinivas, G.S. Kumar, S.V. Suryanarayana, Synthesis and physical properties of $Bi_5Ti_3MnO_{15}$, Solid State Commun. 104 (12) (1997) 741–746.
[12] M.B. Suresh, E.V. Ramana, S.N. Babu, S.V. Suryanarayana, Comparison of electrical and dielectric properties of BLSF materials in Bi–Fe–Ti–O and Bi–Mn–Ti–O systems, Ferroelectrics 332 (2006) 57–63.
[13] A.B. Missyul, I.A. Zvereva, T.T.M. Palstra, A.I. Kurbakov, Double-layered Aurivillius-type ferroelectrics with magnetic moments, Mater. Res. Bull. 45 (2010) 546–550.
[14] Y. Shimakawa, Y. Kubo, Crystal structures and ferroelectric properties of $SrBi_2Ta_2O_9$ and $Sr_{0.8}Bi_{2.2}Ta_2O_9$, Appl. Phys. Lett. 74 (1999) 1904–1906.
[15] Y. Noguchi, T. Goto, M. Miyayama, A. Hoshikawa, T. Kamiyama, Ferroelectric distortion and electronic structure in $Bi_4Ti_3O_{12}$, J. Electroceram. 21 (2008) 49–54.
[16] L. Fuentes, M. Garcia, D. Bueno, M.E. Fuentes, Magnetoelectric effect in $Bi_5Ti_3FeO_{15}$ ceramics obtained by molten salts synthesis, Ferroelectrics 336 (2006) 81.
[17] F. Xia, X. Wang, L. Zhang, X. Yao, Dielectric and piezoelectric properties of PMN-PT ceramics prepared by molten salt synthesis, Ferroelectrics 215 (1998) 181–186.
[18] Zulhadjri, B. Prijamboedi, A.A. Nugroho, Ismunandar, Synthesis and structure analysis of Aurivillius phases $Pb_{1-x}Bi_{4+x}Ti_{4-x}Mn_xO_{15}$, J. Chin. Chem. Soc. 56 (6) (2009) 1108–1111.
[19] A. Fajar, T.H. Priyanto, Santoso, H. Mugirahardjo, N. Suparno, A. Purwanto, Scientific review: neutron diffraction activities in Serpong, Neutron News 18 (2007) 13–18.
[20] B.A. Hunter, C.J. Howard, A computer program for Rietveld analysis of X-ray and neutron powder diffraction patterns, Lucas Heights Research Laboratories, NSW, Australia, 2000, pp. 1–27.
[21] T.Y. Ko, C.H. Jun, J.S Lee, A combined Rietveld refinement on the crystal structure of a magnetoelectric Aurivillius phase $Bi_5Ti_3FeO_{15}$ using neutron and X-ray powder diffraction, Korean J. Ceram. 5 (4) (1999) 341–347.
[22] B.J Kennedy, Q. Zhou, Ismunandar, Y. Kubota, K. Kato, Cation disorder and phase transitions in the four-layer ferroelectric Aurivillius phases $ABi_4Ti_4O_{15}$ ($A=$Ca, Sr, Ba, Pb), J. Solid State Chem. 181 (2008) 1377–1386.
[23] P. Lightfoot, C.H. Hervoches, Structure and phase transitions in Aurivillius phase ferroelectrics, in: Proceedings of the 10th International Ceramics Congress, vol. 10, 2003, pp. 623–630.
[24] N. Niizeki, M. Wachi, The crystal structure of $Bi_2Mn_4O_{10}$, $Bi_2Al_4O_9$ and $Bi_2Fe_4O_9$, Z. Kristallogr. Kristallgeometrie, Kristallphys. Kristallchem. (−144, 1977) 127 (1968) 173–187.
[25] R.D. Shannon, Revised effective ionic radii and systematic studies of interatomic distances in halides and chalcogenides, Acta Crystallogr. A32 (1976) 751–767.
[26] A.M. Glazer, The classification of tilted octahedra in perovskite, Acta Crystallogr. B 28 (1972) 3384–3392.
[27] K.S. Aleksandrov, J. Bartolome, Octahedral tilt phases in perovskite-like crystals with slabs containing an even number of octahedral layers, J. Phys.: Condens. Matter 6 (1994) 8219–8235.
[28] S.K. Sharma, P. Kumar, R. Kumar, M. Knobel, P. Thakur, K.H. Chae, W.K. Choi, R. Kumar, D. Kanjilal, Local structure, optical and magnetic studies of Ni nanostructures embedded in a SiO_2 matrix by ion implantation, J. Phys.: Condens. Matter 20 (2008) 285211.
[29] M. Ikezaki, Y. Noguchi, M. Miyayama, Electrical properties of superlattice-structured $Bi_4Ti_3O_{12}$-$PbBi_4Ti_4O_{15}$ single crystals, J. Am. Ceram. Soc. 90 (9) (2007) 2814–2818.
[30] Ismunandar, B.A. Hunter, B.J. Kennedy, Cation disorder in the ferroelectric Aurivillius phase $PbBi_2Nb_2O_9$: an anomalous dispersion X-ray diffraction study, Solid State Ionics 112 (1998) 281–289.
[31] W.Q. Ni, X.H. Zheng, J.C. Yu, Sintering effects on structure and dielectric properties of dielectrics $CaCu_3Ti_4O_{12}$, J. Mater. Sci. 42 (2007) 1037–1041.